THE JOURNAL OF PHYSICAL CHEMISTRY A

Article

Cite This: J. Phys. Chem. A 2019, 123, 2843−2852

pubs.acs.org/JPCA

Halide Ion Microhydration: Structure, Energetics, and Spectroscopy of Small Halide−Water Clusters

Pushp Bajaj,*[,†] Marc Riera,[†] Jason K. Lin,[†] Yaira E. Mendoza Montijo,[†] Jessica Gazca,[†] and Francesco Paesani*[,†,‡,§]

[†]Department of Chemistry and Biochemistry, [‡]Materials Science and Engineering, and [§]San Diego Supercomputer Center, University of California San Diego, La Jolla, California 92093, United States

Supporting Information

ABSTRACT: Replica exchange molecular dynamics simulations and vibrational spectroscopy calculations are performed using halide−water many-body potential energy functions to provide a bottom-up analysis of the structures, energetics, and hydrogen-bonding arrangements in $X^-(H_2O)_n$ (n = 3−6) clusters, with X = F, Cl, Br, and I. Independently of the cluster size, it is found that all four halides prefer surface-type structures in which they occupy one of the vertices in the underlying three-dimensional hydrogen-bond networks. For fluoride−water clusters, this is in contrast to previous reports suggesting that fluoride prefers interior-type arrangements, where the ion is fully hydrated. These differences can be ascribed to the variability in how various molecular models are capable of reproducing the subtle interplay between halide−water and water−water interactions. Our results thus emphasize the importance of a correct representation of individual many-body contributions to the molecular interactions for a quantitative description of halide ion hydration.

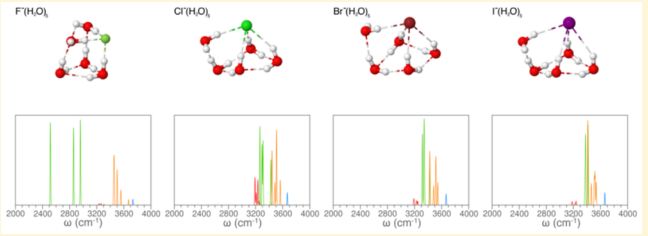

INTRODUCTION

Determining the properties of ionic solutions in different environments is a long-sought-after goal in the physical sciences. Ionic solutions are ubiquitous in nature and mediate fundamental chemical, biological, environmental, and industrial processes.[1−8] For instance, alkali and alkaline earth metal ions, such as Na^+, K^+, Ca^{2+}, and Mg^{2+}, play an important role in biological processes that are responsible for the rigidity and hardness of bones and teeth, blood clotting, muscle contraction, and transport of water and nutrients through cell membranes, to name a few.[3,5] In the atmosphere, ions dissolved in sea-spray aerosol (SSA) modulate the hygroscopicity, chemical reactivity, and gas uptake ability of SSA particles,[9−12] which alter particle size and chemical composition and, in turn, affect the ability of the same particles to scatter solar radiation and act as cloud and ice condensation nuclei.[13] In materials science, ionic solutions are a crucial part of devices such as electrolytic cells, capacitors, and batteries.[2]

The properties of ionic solutions directly depend on how ions perturb the structure and dynamics of the surrounding water hydrogen-bond (H-bond) network. Although some qualitative correlations can be established between an ion's charge density and electronegativity and the strength of water−water H-bonds, a quantitative understanding of the magnitude and extent to which specific ions disrupt or strengthen the water H-bond network is yet to be achieved.[4,14] In this context, studies of small gas-phase ionic clusters can provide molecular level insights into the fundamental questions regarding the strength of the underlying molecular interactions, H-bond arrangements, and reactivity.[15] Small clusters are also amenable to high-level ab initio electronic structure calculations that are typically computationally unaffordable for bulk solutions, which makes clusters ideal systems to test and validate molecular models of ion−water interactions.[16,17] Additionally, studying ion−water clusters of increasing size provides a systematic bottom-up approach to understanding ion hydration, one water molecule at a time.

Over the past two decades, several computational studies focused on determining the structures, relative energies, and vibrational spectra of aqueous ionic clusters.[18−24] The molecular modeling of the hydration of halide ions is particularly challenging since halide−water H-bonds can perturb, in a nontrivial way, both the structure and dynamics of the surrounding water H-bond network.[15] Moreover, the strength of the halide−water interactions varies significantly as a function of ion size, charge density, and polarizability. Early theoretical investigations used ab initio density functional theory (DFT) and perturbation theory methods (e.g., MP2) to characterize both the structure and energetics of small halide−water clusters.[18−21,25,26] Pioneering molecular dynamics (MD) simulations of halide−water clusters, carried out with polarizable force fields (FFs), found that all halide ions except fluoride prefer to be located at the surface of water clusters.[27−30] On the other hand, analogous simulations

Received: January 26, 2019
Revised: March 10, 2019
Published: March 11, 2019

DOI: 10.1021/acs.jpca.9b00816
J. Phys. Chem. A 2019, 123, 2843−2852

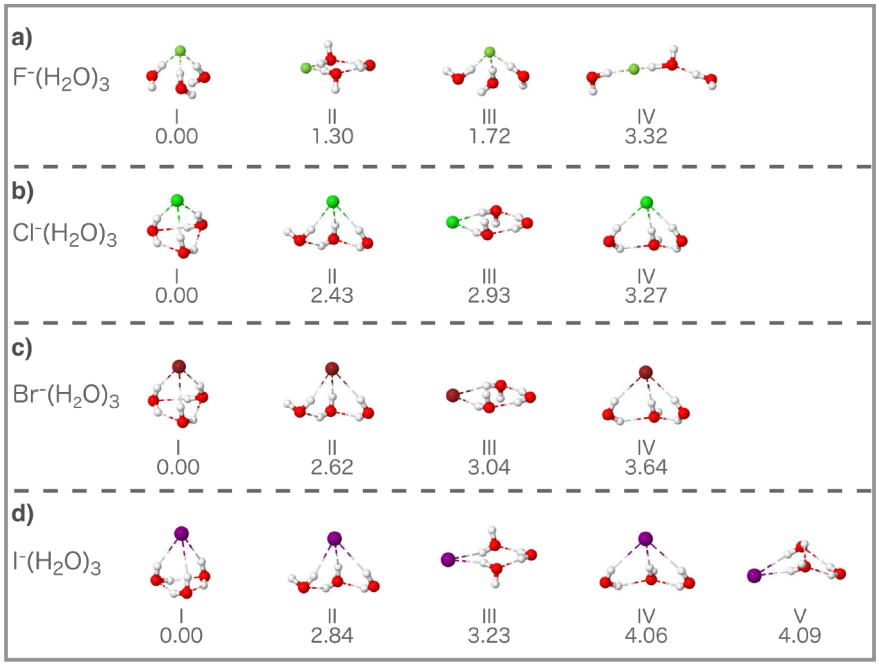

Figure 1. Minimum energy structural isomers along with their relative binding energies (in kcal/mol) of $F^-(H_2O)_3$ (a), $Cl^-(H_2O)_3$ (b), $Br^-(H_2O)_3$ (c), and $I^-(H_2O)_3$ (d) clusters.

carried out with nonpolarizable FFs predicted all halide ions to prefer the interior of the clusters, thus emphasizing the importance of many-body effects in ion−water interactions.[31−33] More recently, the development of many-body potential energy functions, rigorously derived from high-level ab initio data, has facilitated studies of small gas-phase clusters through molecular dynamics (MD) simulations and vibrational spectra calculations which can directly be compared with corresponding experimental measurements.[34−39] The results of these studies show a large degree of variability which depend sensitively on the molecular models used in the simulations and the subtle competition between ion−water and water−water interactions, which are further modulated by nuclear quantum effects.

In this study, we provide insights into the interplay between halide−water and water−water H-bond strengths and arrangements in halide−water clusters through the analysis of the corresponding structures and associated vibrational spectra. Specifically, replica exchange molecular dynamics (REMD) simulations of $X^-(H_2O)_n$ clusters, with X = F, Cl, Br, and I and n = 3−6, are performed using the MB-nrg many-body potential energy functions (PEFs) introduced in refs 37 and 38. Several low-lying energy isomers of each $X^-(H_2O)_n$ cluster are identified and further characterized from calculations of anharmonic vibrational spectra. Finally, isomeric equilibria for each $X^-(H_2O)_n$ cluster are determined, which allows us to monitor the evolution of the H-bond network as a function of temperature, thus providing a systematic approach to understanding the hydration of halide ions in systems with increasing size and complexity.

COMPUTATIONAL METHODS

All calculations are carried out with the MB-nrg PEFs introduced in ref 37 which describe the underlying molecular interactions through rigorous representations of individual many-body terms. Within the MB-nrg framework, all water−water interactions are represented by the MB-pol PEFs that have been shown to accurately predict the properties of water across all phases.[40−44] The halide−water interactions are described by a two-body term, which is expressed through the combination of a short-range permutationally invariant polynomial and a classical description of permanent electrostatics and dispersion energy, along with a many-body term represented by classical polarization.

Following previous studies of thermodynamic equilibria in small aqueous clusters, classical replica exchange molecular dynamics (REMD) simulations are carried out to identify the low-lying isomers of $X^-(H_2O)_n$ clusters, with n = 3−6 and X = F, Cl, Br, and I. Specifically, 64 replicas in the temperature range from 10 to 200 K are used for both $X^-(H_2O)_3$ and $X^-(H_2O)_4$ clusters, 64 replicas in the temperature range from 20 to 150 K are used for the $X^-(H_2O)_5$ clusters, and 96 replicas in the temperature range from 20 to 200 K are used for the $X^-(H_2O)_6$ clusters. For each cluster size, the replicas are distributed according to a geometric temperature progression, $T_i = T_0 e^{\Delta(i-1)}$, where T_i is the temperature of the ith replica, T_0 is the temperature of the first replica, Δ is a constant, and i is the number of the ith replica. The number of replicas and the temperature range are determined to optimize both the computational cost and the sampling efficiency of the underlying free-energy surfaces. All REMD simulations were carried using an in-house C++ code. Molecular configurations are extracted from the REMD simulation trajectories at regular time intervals, and optimized to identify low-lying structural isomers of all the $X^-(H_2O)_n$ clusters, using an interatomic distance based root-mean-square deviation (RMSD) criterion.

To characterize the influence of the halide ions on the evolution of the water H-bond network as a function of cluster size, the intramolecular vibrational frequencies of the water molecules are calculated using a combined local-mode[45,46] and local-monomer[47] (LM) approach, as described in refs 48 and 49. The Hessian matrix is computed at the optimized geometry of each isomer from finite differentiation of analytic first derivatives obtained with MB-nrg PEFs. Local modes[45,46,50]

DOI: 10.1021/acs.jpca.9b00816
J. Phys. Chem. A 2019, 123, 2843−2852

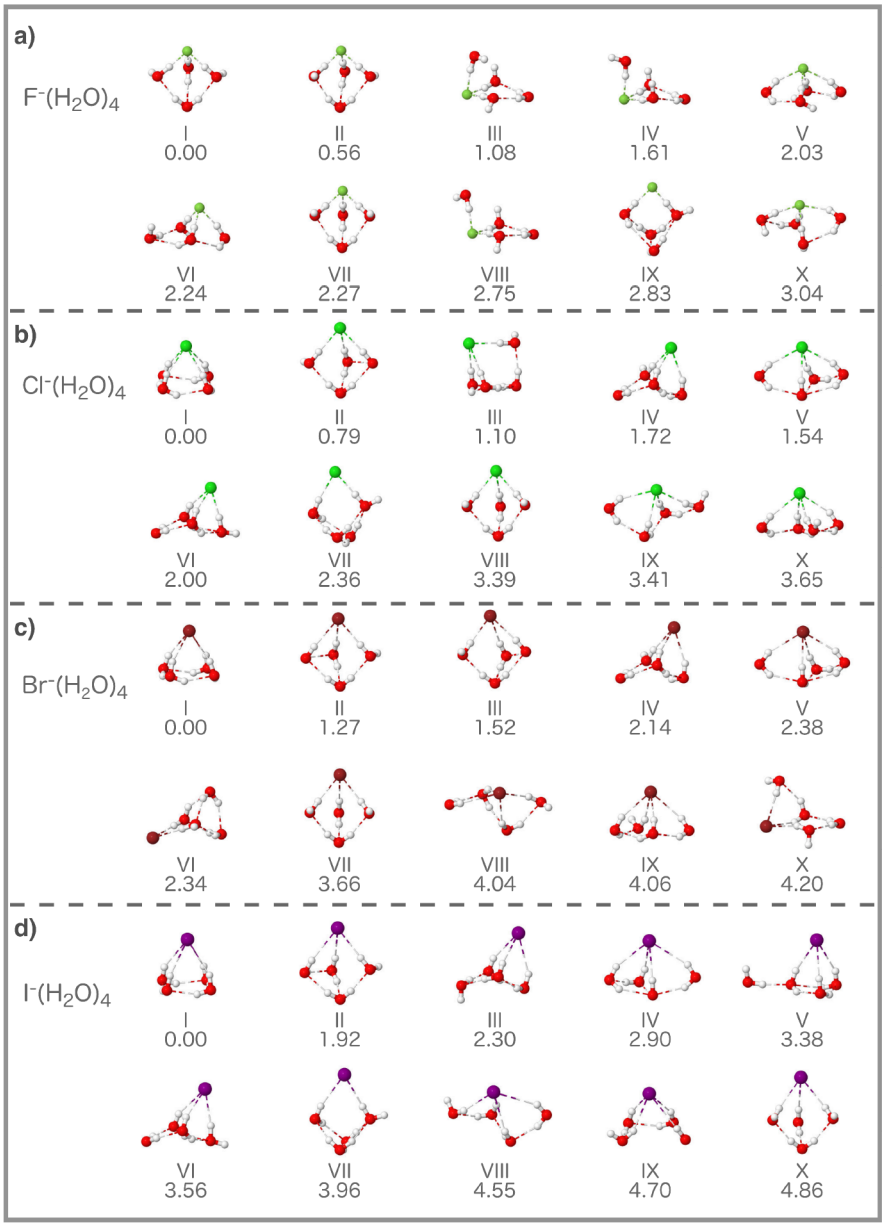

Figure 2. Minimum energy structural isomers along with their relative binding energies (in kcal/mol) of $F^-(H_2O)_4$ (a), $Cl^-(H_2O)_4$ (b), $Br^-(H_2O)_4$ (c), and $I^-(H_2O)_4$ (d) clusters.

are then created using a distance-based (Boys) localization scheme in a frequency window of 500 cm^{-1}. The three highest-frequency modes, corresponding to the two stretching modes and one bending mode of a water molecule, are identified and used to integrate the potential energy using Gauss−Hermite quadrature on a grid of nine points in each dimension. The "local-monomer" Hamiltonian[51,52] is diagonalized in this reduced three-dimensional space composed of the local modes for each water monomer to yield anharmonic eigenfrequencies and eigenvectors. Since, for each quadrature grid point, the potential energy is evaluated for the whole cluster, environmental effects are included in the calculations, to some extent.

RESULTS AND DISCUSSION

The lowest-energy isomers of the $X^-(H_2O)_n$ clusters, with n = 3−6 and X = F, Cl, Br, and I, are shown in Figures 1−4. Independently of the size, all clusters containing the heavier halide ions (i.e., Cl^-, Br^-, and I^-) display similar H-bonding arrangements. Given their relatively larger sizes, these halide ions can accommodate a larger number of water molecules in their first hydration shells, which are arranged to optimize both the number and strength of the water−water H-bonds. As a result, the minimum-energy isomers of all chloride−, bromide−, and iodide−water clusters are characterized by greater number of total (halide−water and water−water) H-bonds than the corresponding fluoride−water clusters, which, on the other hand, exhibit qualitatively different structural motifs, as previously determined from experimental investigations using vibrational predissociation spectroscopy.[15] Due to its small size and consequently larger charge density, the fluoride ion can form stronger H-bonds that effectively "pin" the water molecules in specific three-dimensional arrangements while, at the same time, weakening, when present, the water−water H-bonds in the first hydration shell. The key role played by the

DOI: 10.1021/acs.jpca.9b00816
J. Phys. Chem. A 2019, 123, 2843−2852

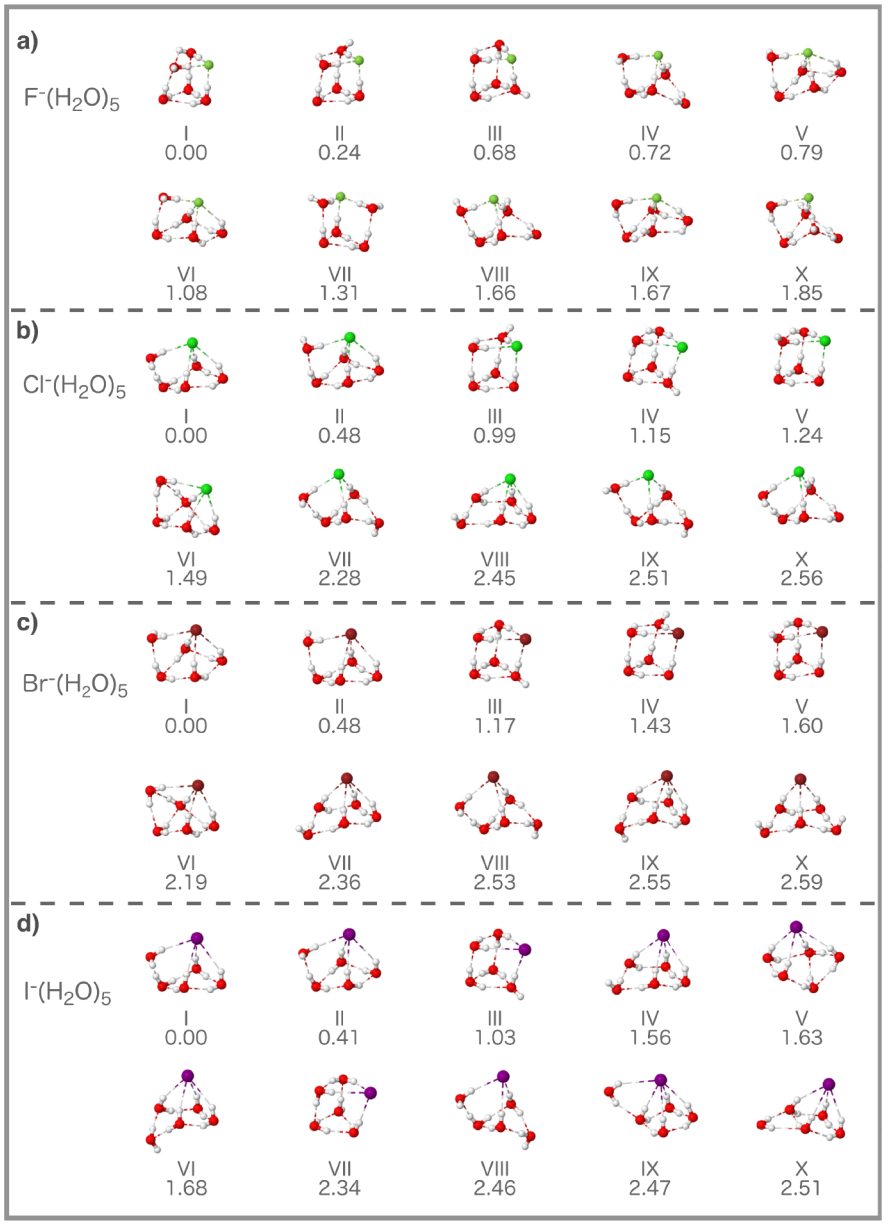

Figure 3. Minimum energy structural isomers along with their relative binding energies (in kcal/mol) of $F^-(H_2O)_5$ (a), $Cl^-(H_2O)_5$ (b), $Br^-(H_2O)_5$ (c), and $I^-(H_2O)_5$ (d) clusters.

fluoride ion in templating the overall structure of the clusters is particularly evident in the lowest-energy isomer of the $F^-(H_2O)_3$ cluster where the water molecules are arranged to optimize the relatively stronger and shorter fluoride−water H-bonds instead of forming water−water H-bonds.

It should be noted that many isomers of all four halide−water clusters, particularly those with larger *N*, can be interconverted into each other by rotation of one or two water molecules. Although these rotations are accompanied by only minor changes in the overall H-bonding topology of the clusters, they lead to isomers that are significantly different in energy (by up to ∼0.7 kcal/mol). This suggests that the interplay between cooperative and anticooperative effects may be responsible for the relative stability of different H-bonding arrangements. In this context, a recent analysis of small halide−water clusters carried out using the ALMO-EDA method[53,54] demonstrated that the nature of the interactions of fluoride with water is distinctively different from those of the other halides.[55] Notably, energy decompositions calculated with hybrid functionals of halide−water dimers showed that polarization and charge transfer energies of $F^-(H_2O)$ made up around 102% of the total interaction energy (with the other remaining terms canceling each other out), whereas polarization and charge transfer made up around 60, 55, and 49% of chloride−, bromide−, and iodide−water dimer interaction energies, respectively. Additionally, energy decompositions of stable halide−water trimers demonstrated strong anticooperativity (approximately +3.0 and +1.8 kcal/mol in the three-body polarization and charge transfer terms, respectively) associated with the fluoride ion accepting hydrogen bonds from two water molecules, while three-body polarization and charge transfer together contribute approximately +1.1, +0.7, and +0.3 kcal/mol in the chloride, bromide, and iodide trimers having similar hydrogen bonding structures.[55]

One aspect that is often debated in the literature is whether halide ions prefer to reside at the surface or in the interior of

DOI: 10.1021/acs.jpca.9b00816
J. Phys. Chem. A 2019, 123, 2843−2852

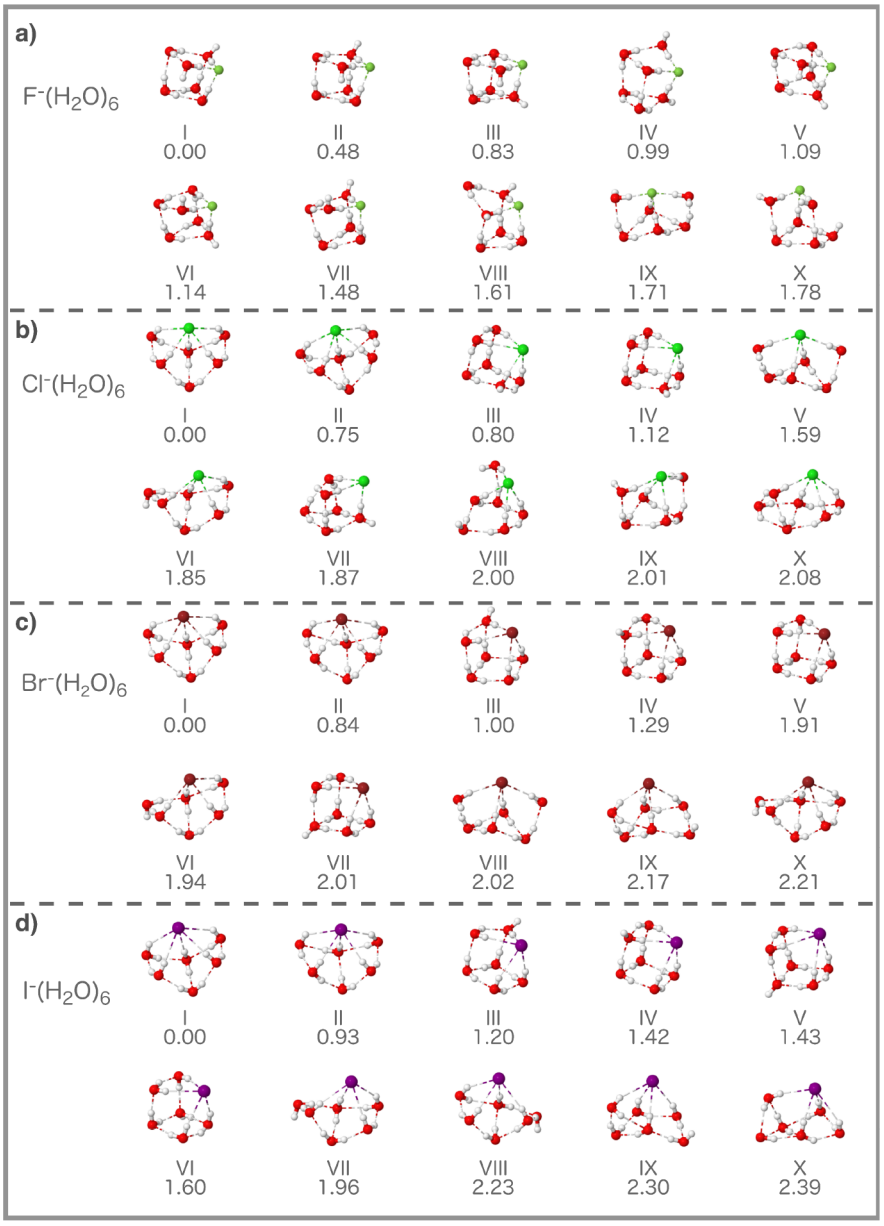

Figure 4. Minimum energy structural isomers along with their relative binding energies (in kcal/mol) of $F^-(H_2O)_6$ (a), $Cl^-(H_2O)_6$ (b), $Br^-(H_2O)_6$ (c), and $I^-(H_2O)_6$ (d) clusters.

water clusters and how this preference varies as a function of temperature and cluster size.[18−21,25−33] It is commonly found that the lowest-energy arrangements of fluoride−water clusters correspond to interior-type structures, where the fluoride ion can be fully solvated, while the corresponding clusters containing the heavier halide ions tend to prefer three-dimensional arrangements with the ion located at the surface. The different behavior between F^- on one side and Cl^-, Br^-, and I^- on the other side is generally attributed to the more pronounced covalent character of the fluoride ion that can thus establish relatively stronger interactions with the surrounding water molecules. However, a conclusive agreement on the possible structural isomers and their relative stability has not yet been reached.[26] In the present analysis, no interior-type structures are found among the 10 lowest-energy isomers of the $X^-(H_2O)_n$ with n = 3−6 reported in Figures 1−4. As mentioned above, the relative stability of the different isomers depends on the subtle competition between halide−water and water−water intermolecular interactions. In this context, it has been shown that calculation carried out with different DFT models and/or small basis sets produce significant cluster-dependent errors in binding energies, many-body interaction energies, and vibrational frequencies in pure water, cation−water, and anion−water clusters.[16,17,37,43,56−59] In several cases, it was found that the apparent agreement between approximate models and high-quality reference data for ion−water interactions is mainly due to significant error cancellation among individual terms of the corresponding many-body expansion of the interaction energy. It is important to note that a key factor that affects the calculated energy ordering of different isomers is the relative accuracy of the model in representing the ion−water and water−water interactions, which, in turn, varies greatly depending on the specific ion and isomer configuration.[17,37,43,56] Among the DFT models, only the most sophisticated range-separated dispersion-corrected hybrid functionals approach chemical accuracy in describing

DOI: 10.1021/acs.jpca.9b00816
J. Phys. Chem. A 2019, 123, 2843−2852

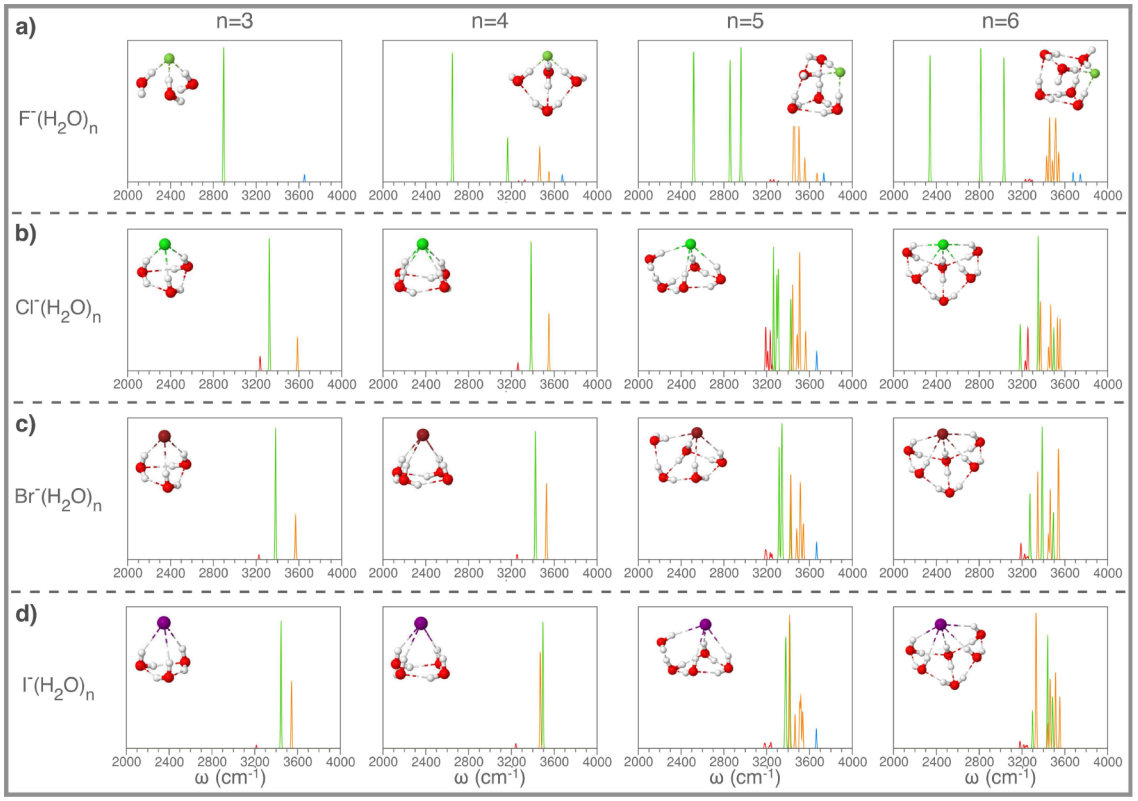

Figure 5. Calculated anharmonic vibrational spectra (in cm^{-1}) of global minimum energy structural isomers of $F^-(H_2O)_n$ (a), $Cl^-(H_2O)_n$ (b), $Br^-(H_2O)_n$ (c), and $I^-(H_2O)_n$ (d) clusters, where n = 3−6. The bend overtones are highlighted in red, the H-bonded-to-ion OH stretches are highlighted in green, the H-bonded-to-water OH stretches are highlighted in orange, and the free OH stretches are highlighted in blue.

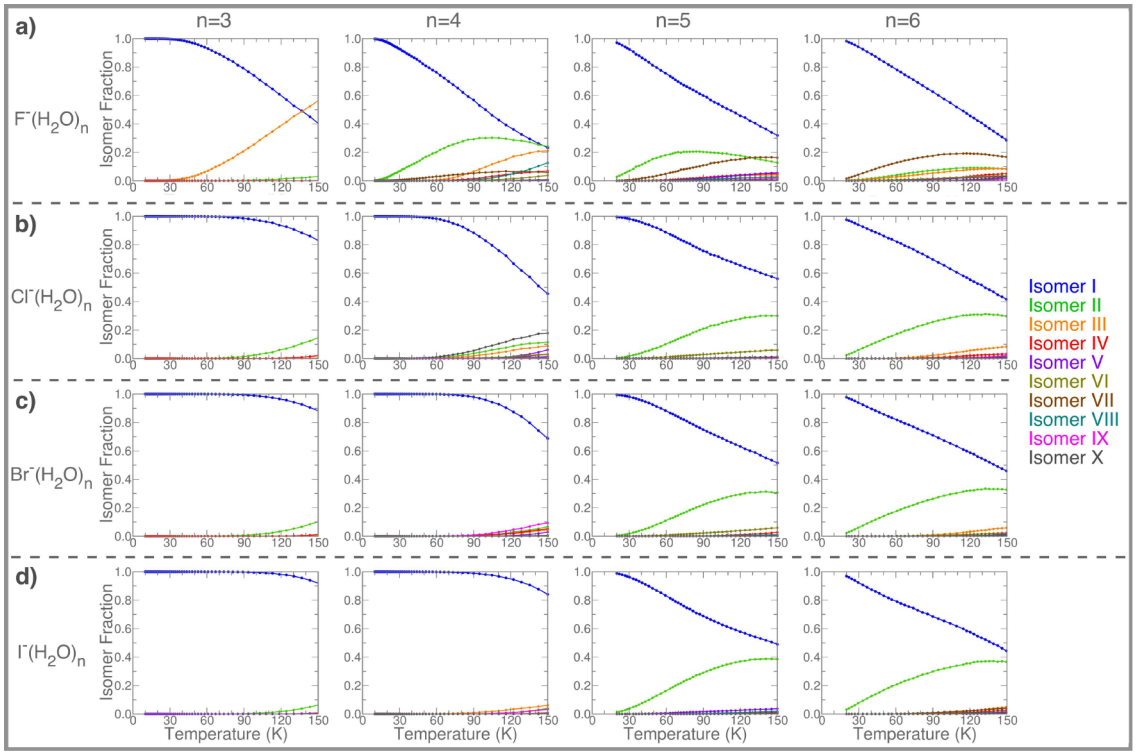

Figure 6. Temperature dependent relative populations of minimum energy isomers for $F^-(H_2O)_n$ (a), $Cl^-(H_2O)_n$ (b), $Br^-(H_2O)_n$ (c), and $I^-(H_2O)_n$ (d) clusters, where n = 3−6.

many-body ion−water interactions.[17,56] However, such functionals are rarely employed in extensive analysis of stable structures of ion−water clusters and MD simulations due to the prohibitively high associated computational cost.

DOI: 10.1021/acs.jpca.9b00816
J. Phys. Chem. A 2019, 123, 2843−2852

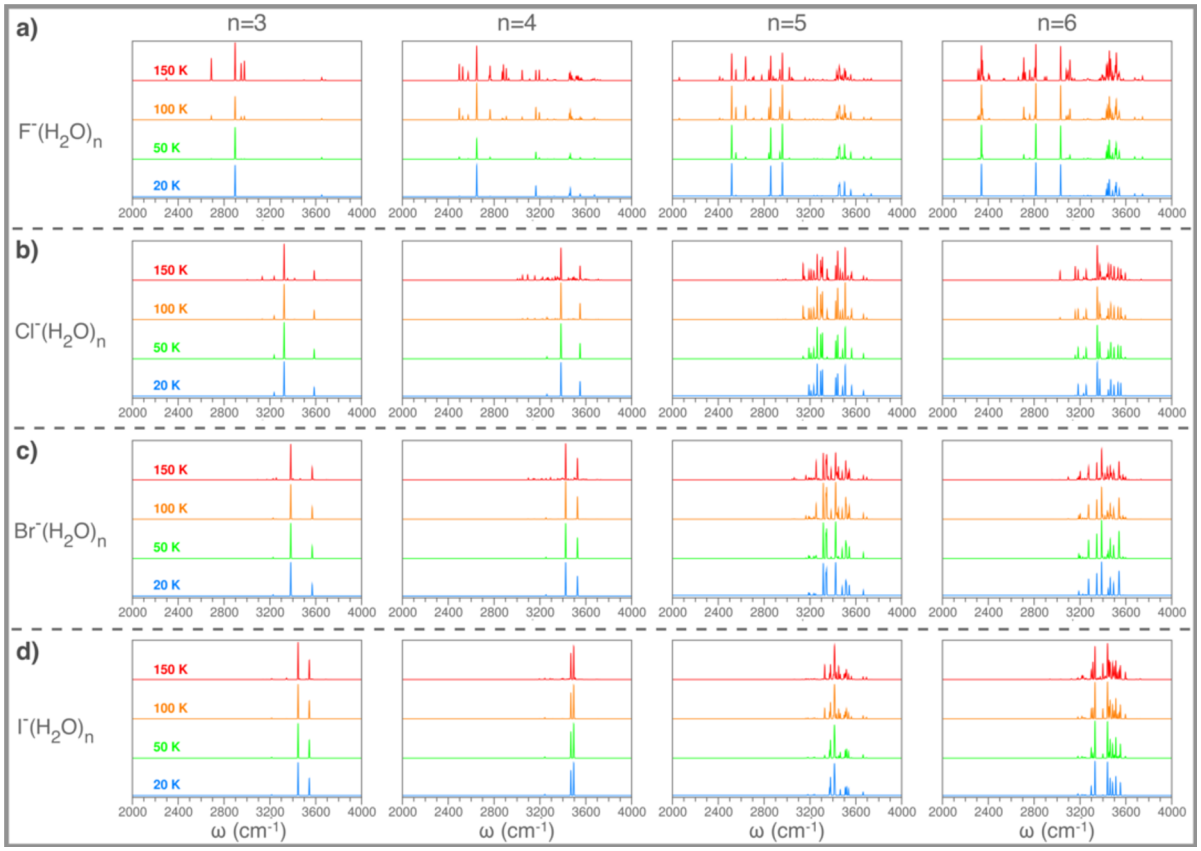

Figure 7. Finite temperature anharmonic spectra (in cm^{-1}) obtained by weighting the individual calculated spectrum of the minimum energy isomers (Figures 1–4) with their corresponding temperature dependent populations (Figure 6), for $F^-(H_2O)_n$ (a), $Cl^-(H_2O)_n$ (b), $Br^-(H_2O)_n$ (c), and $I^-(H_2O)_n$ (d) clusters, where n = 3–6. Spectra were calculated at four different temperatures: 20 (blue), 50 (green), 100 (orange), and 150 K (red).

To provide further insights into the nature of halide–water interactions in $X^-(H_2O)_n$ clusters, with n = 3–6, anharmonic infrared spectra of the lowest-energy isomers (global minima) are calculated using the LM approach. The calculated spectra, shown in Figure 5 in the frequency region associated with OH stretching vibrations, are a direct probe of the strength of ion–water and water–water interactions in each cluster and allow for comparisons with corresponding experimental measurements. As discussed above, the more pronounced basic character of F^-, which is responsible for relatively stronger H-bonds compared to those formed by the other halide ions, results in qualitatively different cluster structures that are manifested in distinct spectral features. The analysis of Figure 5 shows that the peaks associated with OH-stretch H-bonded to the halide ions (shown in green in Figure 5) move to higher frequencies going from $F^-(H_2O)_n$ clusters to $I^-(H_2O)_n$, which is a clear manifestation of the decreasing strength of the halide–water H-bonds, going from F^- to I^-. On the other hand, the opposite trend is found for the peaks corresponding to OH bonds involved in water–water H-bonds (shown in orange in Figure 5), which lie in the ∼3450–3550 cm^{-1} region. Going from Cl^- to I^-, particularly for clusters containing three and four water molecules, these peaks shift slightly toward lower frequencies indicating increasing strength of the corresponding water–water H-bonds. These trends are consistent with previously reported experimental measurements.[15,60] Importantly, due to more symmetric arrangements of the water molecules in the lowest-energy isomers of $X^-(H_2O)_n$ clusters, with X = Cl, Br, and I, several OH-stretch vibrations are degenerate or nearly degenerate, which results in infrared spectra with peaks closer to each other and spanning narrower frequency ranges. Anharmonic vibrational frequencies for all the other isomers shown in Figures 1–4 are provided in the Supporting Information.

In principle, the calculated spectra shown in Figure 5 can be compared to the corresponding experimental infrared predissociation spectra measured using cold ion traps and "messenger" technique. However, the experimental spectra do not strictly correspond to the spectra shown in Figure 5, which are calculated at 0 K, but report the infrared response associated with a distribution of isomers compatible with the temperature of the measurements. For a one-to-one comparison with finite temperature measurements, the theoretical spectra of the individual isomers must be weighted by the thermal, preferably quantum, distribution at that temperature.[48] In order to study the temperature dependent evolution of the $X^-(H_2O)_n$ clusters, populations of the different isomers calculated from classical REMD simulations in a range of temperatures from 20 to 150 K are reported in Figure 6. Cluster configurations are extracted from the simulation trajectories at regular time intervals and optimized to the nearest local minimum on the potential energy surface. Considering only the positions of the heavy atoms, an RMSD criterion is then used to classify the optimized configuration as one of the low-lying $X^-(H_2O)_n$ isomers shown in Figures 1–4. As expected, the results show that at low temperatures only the lowest energy isomer dominates the equilibrium Boltzmann distribution for each cluster. At higher

DOI: 10.1021/acs.jpca.9b00816
J. Phys. Chem. A 2019, 123, 2843–2852

temperatures, for most chloride−, bromide−, and iodide−water clusters, the next higher energy isomer is found to contribute increasingly to the distribution. Higher energy isomers contribute little to the distribution even at 150 K, except for fluoride−water clusters, where multiple isomers gain comparable populations with increasing temperature.

Rigorously, quantum thermal populations of the different isomers are needed to make quantitative comparisons with experimental measurements. However, since nuclear quantum effects can be approximately mimicked by temperature shifts, the anharmonic vibrational frequencies calculated for the low-lying isomers (Figure 5) combined with the classical thermal populations (Figure 6) provide a qualitative picture of the evolution of the vibrational spectra of halide−water clusters as a function of temperature.[48,49] The vibrational spectra for the $X^-(H_2O)_n$ clusters obtained at 20, 50, 100 and 150 K by weighting the individual anharmonic spectra of the low-lying isomers with their corresponding classical thermal populations are shown in Figure 7. With the exception of $F^-(H_2O)_n$ clusters, for which the temperature-dependent vibrational spectra display features associated with multiple isomers as predicted by the classical thermal populations in Figure 6, the calculated vibrational spectra show very little variation below 100 K, being effectively dominated by the lowest-energy isomer of each $X^-(H_2O)_n$ cluster. Additional spectral features appear at 150 K as the populations of high-energy isomers start to increase (Figure 6). Since the energy differences between different $X^-(H_2O)_n$ isomers are relatively larger than possible differences in the associated zero-point energies, nuclear quantum effects can effectively be accounted for by temperature shifts. It follows that the temperature-dependent vibrational spectra shown in Figure 7 should be good approximations to their quantum counterparts at lower temperatures by ∼20−30 K, which are the temperature shifts generally needed to reproduce nuclear quantum effects in classical MD simulations of aqueous systems.

CONCLUSIONS

Halide−water clusters serve as prototypical model systems for understanding ion hydration, at the molecular level, being the smallest molecular systems where the interplay between halide−water and water−water interactions can be studied in detail. Moreover, a systematic study of increasing cluster sizes provides a bottom-up approach toward investigating bulk ion hydration in condensed phase systems. However, the anharmonic, quantum mechanical halide−water interactions and the competition halide−water and water−water interactions present a challenging problem for theoretical and computational modeling.

In this study, we provided insights into specific ion effects among halide ions from investigations of the H-bond strength and arrangement in $X^-(H_2O)_n$ clusters, with X = F, Cl, Br, and I and n = 3−6. Low-energy isomers of these halide−water clusters were identified through REMD simulations carried out with the MB-nrg PEFs that accurately describe many-body effects in halide−water and water−water interactions. While chloride−, bromide−, and iodide−water clusters exhibit similar structural arrangements, due to similar H-bonding strengths, fluoride−water clusters display qualitatively different configurations, resulting from relatively stronger fluoride−water interactions. In general, all four halide ions prefer exterior positions in the clusters, forming "surface"-type structures where the number and strength of halide−water and water−water H-bonds are optimized. Anharmonic vibrational spectra calculated for the global minimum-energy isomers of all $X^-(H_2O)_n$ clusters were then used as direct probes of different H-bonding arrangements, depending on the halide ion and cluster size. Finally, we characterized the isomeric equilibria as a function of temperature by computing classical populations of the different isomers between 20 and 150 K, and the corresponding temperature-dependent vibrational spectra.

It should be noted that the MB-nrg PEFs used in this study represent many-body interactions through a classical term describing permanent and induced electrostatic effects, which is supplemented with an explicit two-body term that effectively describes nonclassical (two-body) contributions (e.g., charge transfer and penetration, and Pauli repulsion). Future work will focus on the development of explicit three-body representations within the MB-nrg formalism as well as on the investigation of three-body effects on the relative stabilities of different isomers of small $X^-(H_2O)_n$ clusters.

ASSOCIATED CONTENT

Supporting Information

The Supporting Information is available free of charge on the ACS Publications website at DOI: 10.1021/acs.jpca.9b00816.

Cartesian coordinates (in Å) and anharmonic vibrational frequencies (in cm^{-1}) of all isomers of the $X^-(H_2O)_n$ clusters (X = F, Cl, Br, and I; n = 3−6) examined in this study (ZIP)

AUTHOR INFORMATION

Corresponding Authors

*E-mail: pbajaj@ucsd.edu.
*E-mail: fpaesani@ucsd.edu.

ORCID

Francesco Paesani: 0000-0002-4451-1203

Notes

The authors declare no competing financial interest.

ACKNOWLEDGMENTS

We thank Dr. John Kelly for useful discussions about the vibrational spectroscopy of the $X^-(H_2O)_n$ clusters. This research was supported by the National Science Foundation through Grants CHE-1305427 and CHE-1453204. All calculations used resources of the Extreme Science and Engineering Discovery Environment (XSEDE),[61] which is supported by the National Science Foundation through Grant ACI-1053575, under allocation TG-CHE110009, the High Performance Computing Modernization Program (HPCMP) through Grant FA9550-16-1-0327 by the Air Force Office of Scientific Research, and the Triton Shared Computing Cluster (TSCC) at the San Diego Supercomputer Center. M.R. was supported by a Software Fellowship from the Molecular Sciences Software Institute, which is funded by the National Science Foundation through Grant ACI-1547580. Y.E.M.M. and J.G. were supported through the ENLACE summer research program at UC San Diego.

REFERENCES

(1) Knipping, E. M.; Lakin, M. J.; Foster, K. L.; Jungwirth, P.; Tobias, D. J.; Gerber, R. B.; Dabdub, D.; Finlayson-Pitts, B. J. Experiments and Simulations of Ion-Enhanced Interfacial Chemistry on Aqueous NaCl Aerosols. *Science* **2000**, *288*, 301.

DOI: 10.1021/acs.jpca.9b00816
J. Phys. Chem. A 2019, 123, 2843−2852

(2) Winter, M.; Brodd, R. J. What Are Batteries, Fuel Cells, and Supercapacitors? *Chem. Rev.* **2004**, *104*, 4245.
(3) Collins, K. D.; Neilson, G. W.; Enderby, J. E. Ions in Water: Characterizing the Forces That Control Chemical Processes and Biological Structure. *Biophys. Chem.* **2007**, *128*, 95−104.
(4) Marcus, Y. Effect on Ions on the Structure of Water: Structure Making and Breaking. *Chem. Rev.* **2009**, *109*, 1346−1370.
(5) Kunz, W. Specific Ion Effects in Colloidal and Biological Systems. *Curr. Opin. Colloid Interface Sci.* **2010**, *15*, 34−39.
(6) Tobias, D. J.; Stern, A. C.; Baer, M. D.; Levin, Y.; Mundy, C. J. Simulation and Theory of Ions at Atmospherically Relevant Aqueous Liquid-Air Interfaces. *Annu. Rev. Phys. Chem.* **2013**, *64*, 339−359.
(7) Etacheri, V.; Marom, R.; Elazari, R.; Salitra, G.; Aurbach, D. Challenges in the Development of Advanced Li-ion Batteries: a Review. *Energy Environ. Sci.* **2011**, *4*, 3243.
(8) Jungwirth, P.; Cremer, P. S. Beyond Hofmeister. *Nat. Chem.* **2014**, *6*, 261−263.
(9) Forestieri, S. D.; Cornwell, G. C.; Helgestad, T. M.; Moore, K. A.; Lee, C.; Novak, G. A.; Sultana, C. M.; Wang, X.; Bertram, T. H.; Prather, K. A.; et al. Linking Variations in Sea Spray Aerosol Particle Hygroscopicity to Composition During Two Microcosm Experiments. *Atmos. Chem. Phys.* **2016**, *16*, 9003−9018.
(10) Estillore, A. D.; Morris, H. S.; Or, V. W.; Lee, H. D.; Alves, M. R.; Marciano, M. A.; Laskina, O.; Qin, Z.; Tivanski, A. V.; Grassian, V. H. Linking Hygroscopicity and the Surface Microstructure of Model Inorganic Salts, Simple and Complex Carbohydrates, and Authentic Sea Spray Aerosol Particles. *Phys. Chem. Chem. Phys.* **2017**, *19*, 21101−21111.
(11) Hudait, A.; Allen, M. T.; Molinero, V. Sink or Swim: Ions and Organics at the Ice-Air Interface. *J. Am. Chem. Soc.* **2017**, *139*, 10095−10103.
(12) Kelleher, P. J.; Menges, F. S.; DePalma, J. W.; Denton, J. K.; Johnson, M. A.; Weddle, G. H.; Hirshberg, B.; Gerber, R. B. Trapping and Structural Characterization of the $XNO_2{\cdot}NO_3^-$ (X = Cl, Br, I) Exit Channel Complexes in the Water-Mediated $X^- + N_2O_5$ Reactions with Cryogenic Vibrational Spectroscopy. *J. Phys. Chem. Lett.* **2017**, *8*, 4710−4715.
(13) Cochran, R. E.; Ryder, O. S.; Grassian, V. H.; Prather, K. A. Sea Spray Aerosol: The Chemical Link Between the Oceans, Atmosphere, and Climate. *Acc. Chem. Res.* **2017**, *50*, 599−604.
(14) Bakker, H.; Kropman, M.; Omta, A. Effect of Ions on the Structure and Dynamics of Liquid Water. *J. Phys.: Condens. Matter* **2005**, *17*, S3215.
(15) Robertson, W. H.; Johnson, M. A. Molecular Aspects of Halide Ion Hydration: The Cluster Approach. *Annu. Rev. Phys. Chem.* **2003**, *54*, 173−213.
(16) Arismendi-Arrieta, D. J.; Riera, M.; Bajaj, P.; Prosmiti, R.; Paesani, F. i-TTM Model for Ab Initio-Based Ion-Water Interaction Potentials. 1. Halide-Water Potential Energy Functions. *J. Phys. Chem. B* **2016**, *120*, 1822.
(17) Riera, M.; Mardirossian, N.; Bajaj, P.; Götz, A. W.; Paesani, F. Toward Chemical Accuracy in the Description of Ion-Water Interactions Through Many-Body Representations. Alkali-Water Dimer Potential Energy Surfaces. *J. Chem. Phys.* **2017**, *147*, 161715.
(18) Combariza, J. E.; Kestner, N. R.; Jortner, J. Energy-Structure Relationships for Microscopic Solvation of Anions in Water Clusters. *J. Chem. Phys.* **1994**, *100*, 2851.
(19) Baik, J.; Kim, H. M.; Majumdar, D.; Kim, K. S. Structures, Energetics, and Spectra of Fluoride-Water Clusters $F^-(H_2O)_n$, n = 1−6: Ab Initio Study. *J. Chem. Phys.* **1999**, *110*, 9116−9127.
(20) Kim, J.; Lee, H. M.; Suh, S. B.; Majumdar, D.; Kim, K. S. Comparative Ab Initio Study of the Structures, Energetics and Spectra of $X^-{\cdot}(H_2O)_{n=1-4}$ [X = F, Cl, Br, I] clusters. *J. Chem. Phys.* **2000**, *113*, 5259−5272.
(21) Lee, H. M.; Kim, D.; Kim, K. S. Structures, Spectra, and Electronic Properties of Halide-Water Pentamers and Hexamers, $X^-(H_2O)_{5,6}$ (X = F, Cl, Br, I): *Ab Initio* Study. *J. Chem. Phys.* **2002**, *116*, 5509.
(22) Yoo, S.; Lei, Y. A.; Zeng, X. C. Effect of Polarizability on the Ionic Solvation in Water Clusters. *J. Chem. Phys.* **2003**, *119*, 6083.
(23) Ayala, R.; Martinez, J. M.; Pappalardo, R. R.; Marcos, E. S. Study of the Stabilization Energies of Halide−Water Clusters: An Application of First-Principles Interaction Potentials Based on a Polarizable and Flexible Model. *J. Chem. Phys.* **2004**, *121*, 7269.
(24) Tobias, D. J.; Jungwirth, P.; Parrinello, M. Surface Solvation of Halogen Anions in Water Clusters: An *Ab Initio* Molecular Dynamics Study of the $Cl^-(H_2O)_6$ Complex. *J. Chem. Phys.* **2001**, *114*, 7036.
(25) Xantheas, S. S. Quantitative Description of Hydrogen Bonding in Chloride-Water Clusters. *J. Phys. Chem.* **1996**, *100*, 9703−9713.
(26) Wen, H.; Huang, T.; Liu, Y.-R.; Jiang, S.; Peng, X.-Q.; Miao, S.-K.; Wang, C.-Y.; Hong, Y.; Huang, W. Structure, Temperature Effect and Bonding Order Analysis of Hydrated Bromide Clusters. *Chem. Phys.* **2016**, *479*, 129−142.
(27) Perera, L.; Berkowitz, M. L. Many-Body Effects in Molecular Dynamics Simulations of $Na^+(H_2O)_n$ and $Cl^-(H_2O)_n$ Clusters. *J. Chem. Phys.* **1991**, *95*, 1954.
(28) Perera, L.; Berkowitz, M. L. Structure and Dynamics of $Cl^-(H_2O)_{20}$ Clusters: The Effect of the Polarizability and the Charge of the Ion. *J. Chem. Phys.* **1992**, *96*, 8288.
(29) Perera, L.; Berkowitz, M. L. Stabilization Energies of Cl^-, Br^-, and I^-Ions in Water Clusters. *J. Chem. Phys.* **1993**, *99*, 4222.
(30) Perera, L.; Berkowitz, M. L. Structures of $Cl^-(H_2O)_n$ and $F^-(H_2O)_n$ (n = 2, 3, ..., 15) Clusters. Molecular Dynamics Computer Simulations. *J. Chem. Phys.* **1994**, *100*, 3085.
(31) Dang, L. X.; Smith, D. E. Molecular Dynamics Simulations of Aqueous Ionic Clusters Using Polarizable Water. *J. Chem. Phys.* **1993**, *99*, 6950.
(32) Stuart, S. J.; Berne, B. J. Effects of Polarizability on the Hydration of the Chloride Ion. *J. Phys. Chem.* **1996**, *100*, 11934−11943.
(33) Stuart, S. J.; Berne, B. J. Surface Curvature Effects in the Aqueous Ionic Solvation of the Chloride Ion. *J. Phys. Chem. A* **1999**, *103*, 10300−10307.
(34) Rheinecker, J.; Bowman, J. M. The Calculated Infrared Spectrum of Cl^-H_2O Using a New Full Dimensional Ab Initio Potential Surface and Dipole Moment Surface. *J. Chem. Phys.* **2006**, *125*, 133206.
(35) Kamarchik, E.; Bowman, J. M. Quantum Vibrational Analysis of Hydrated Ions Using an ab Initio Potential. *J. Phys. Chem. A* **2010**, *114*, 12945−12951.
(36) Wang, X.-G.; Carrington, T., Jr. Rovibrational Levels and Wavefunctions of Cl^-H_2O. *J. Chem. Phys.* **2014**, *140*, 204306.
(37) Bajaj, P.; Götz, A. W.; Paesani, F. Toward Chemical Accuracy in Description of Ion-Water Interactions through Many-Body Representations. I. Halide-Water Dimer Potential Energy Surfaces. *J. Chem. Theory Comput.* **2016**, *12*, 2698−2705.
(38) Bajaj, P.; Wang, X.-G.; Carrington, T., Jr.; Paesani, F. Vibrational Spectra of Halide-Water Dimers: Insights on Ion Hydration from Full-Dimensional Quantum Calculations on Many-Body Potential Energy Surfaces. *J. Chem. Phys.* **2018**, *148*, 102321.
(39) Mallory, J. D.; Mandelshtam, V. A. Nuclear Quantum Effects and Thermodynamics Properties for Small $(H_2O)_{1-21}X^-$Clusters (X^-= F^-, Cl^-, Br^-, I^-). *J. Phys. Chem. A* **2018**, *122*, 4167−4180.
(40) Medders, G. R.; Paesani, F. Infrared and Raman Spectroscopy of Liquid Water through "First-Principles" Many-Body Molecular Dynamics. *J. Chem. Theory Comput.* **2015**, *11*, 1145−1154.
(41) Medders, G. R.; Paesani, F. Dissecting the Molecular Structure of the Air/Water Interface from Quantum Simulations of the Sum-Frequency Generation Spectrum. *J. Am. Chem. Soc.* **2016**, *138*, 3912−3919.
(42) Paesani, F. Getting the Right Answers for the Right Reasons: Toward Predictive Molecular Simulations of Water with Many-Body Potential Energy Functions. *Acc. Chem. Res.* **2016**, *49*, 1844−1851.
(43) Reddy, S. K.; Straight, S. C.; Bajaj, P.; Pham, C. H.; Riera, M.; Moberg, D. R.; Morales, M. A.; Knight, C.; Götz, A. W.; Paesani, F. On the Accuracy of the MB-pol Many-Body Potential for Water: Interaction Energies, Vibrational Frequencies, and Classical Thermo-

DOI: 10.1021/acs.jpca.9b00816
J. Phys. Chem. A 2019, 123, 2843−2852

dynamic and Dynamical Properties from Clusters to Liquid Water and Ice. *J. Chem. Phys.* **2016**, *145*, 194504.
(44) Richardson, J. O.; Pérez, C.; Lobsiger, S.; Reid, A. A.; Temelso, B.; Shields, G. C.; Kisiel, Z.; Wales, D. J.; Pate, B. H.; Althorpe, S. C. Concerted Hydrogen-Bond Breaking by Quantum Tunneling in the Water Hexamer Prism. *Science* **2016**, *351*, 1310.
(45) Cheng, X.; Steele, R. P. Efficient Anharmonic Vibrational Spectroscopy for Large Molecules Using Local-Mode Coordinates. *J. Chem. Phys.* **2014**, *141*, 104105.
(46) Cheng, X.; Talbot, J. J.; Steele, R. P. Tuning Vibrational Mode Localization with Frequency Windowing. *J. Chem. Phys.* **2016**, *145*, 124112.
(47) Wang, Y.; Huang, X.; Shepler, B. C.; Braams, B. J.; Bowman, J. M. Flexible, *Ab Initio* Potential, and Dipole Moment Surfaces for Water. I. Tests and Applications for Clusters up to the 22-mer. *J. Chem. Phys.* **2011**, *134*, 094509.
(48) Brown, S. E.; Götz, A. W.; Cheng, X.; Steele, R. P.; Mandelshtam, V. A.; Paesani, F. Monitoring Water Clusters Melt? Through Vibrational Spectroscopy. *J. Am. Chem. Soc.* **2017**, *139*, 7082−7088.
(49) Riera, M.; Brown, S. E.; Paesani, F. Isomeric Equilibria, Nuclear Quantum Effects, and Vibrational Spectra of $M^+(H_2O)_{n=1;3}$ Clusters, with M = Li, Na, K, Rb, and Cs, through Many-Body Representations. *J. Phys. Chem. A* **2018**, *122*, 5811−5821.
(50) Jacob, C. R.; Reiher, M. Localizing Normal Modes in Large Molecules. *J. Chem. Phys.* **2009**, *130*, 084106.
(51) Wang, Y.; Bowman, J. M. Towards an *Ab Initio* Flexible Potential for Water, and Post-Harmonic Quantum Vibrational Analysis of Water Clusters. *Chem. Phys. Lett.* **2010**, *491*, 1.
(52) Wang, Y.; Bowman, J. M. IR Spectra of the Water Hexamer: Theory, with Inclusion of the Monomer Bend Overtone, and Experiment are in Agreement. *J. Phys. Chem. Lett.* **2013**, *4*, 1104−1108.
(53) Horn, P. R.; Mao, Y.; Head-Gordon, M. Probing Non-Covalent Interactions with a Second Generation Energy Decomposition Analysis Using Absolutely Localized Molecular Orbitals. *Phys. Chem. Chem. Phys.* **2016**, *18*, 23067−23079.
(54) Horn, P. R.; Mao, Y.; Head-Gordon, M. Defining the Contributions of Permanent Electrostatics, Pauli Repulsion, and Dispersion in Density Functional Theory Calculations of Intermolecular Interaction Energies. *J. Chem. Phys.* **2016**, *144*, 114107.
(55) Bizzarro, B. B.; Egan, C. K.; Paesani, F. On the Nature of Halide-Water Interactions: Insights from Many-Body Representations and Density Functional Theory. 2019. https://doi.org/10.26434/chemrxiv.7613042.v2.
(56) Egan, C. K.; Paesani, F. Assessing Many-Body Effects of Water Self-Ions. I: $OH^-(H_2O)_n$ Clusters. *J. Chem. Theory Comput.* **2018**, *14*, 1982−1997.
(57) Cisneros, G. A.; Wikfeldt, K. T.; Ojamäe, L.; Lu, J.; Xu, Y.; Torabifard, H.; Bartók, A. P.; Csányi, G.; Molinero, V.; Paesani, F. Modeling Molecular Interactions in Water: From Pairwise to Many-Body Potential Energy Functions. *Chem. Rev.* **2016**, *116*, 7501−7528.
(58) Howard, J. C.; Enyard, J. D.; Tschumper, G. S. Assessing the Accuracy of Some Popular DFT Methods for Computing Harmonic Vibrational Frequencies of Water Clusters. *J. Chem. Phys.* **2015**, *143*, 214103.
(59) Howard, J. C.; Tschumper, G. S. Benchmark Structures and Harmonic Vibrational Frequencies Near the CCSD(T) Complete Basis Set Limit for Small Water Clusters: $(H_2O)_{n=2,3,4,5,6}$. *J. Chem. Theory Comput.* **2015**, *11*, 2126−2136.
(60) Ayotte, P.; Bailey, C. G.; Weddle, G. H.; Johnson, M. A. Vibrational Spectroscopy of Small $Br^-\cdot(H_2O)_n$ and $I^-\cdot(H_2O)_n$ Clusters: Infrared Characterization of the Ionic Hydrogen Bond. *J. Phys. Chem. A* **1998**, *102*, 3067.
(61) Towns, J.; Cockerill, T.; Dahan, M.; Foster, I.; Gaither, K.; Grimshaw, A.; Hazlewood, V.; Lathrop, S.; Lifka, D.; Peterson, G. D.; et al. XSEDE: Accelerating Scientific Discovery. *Comput. Sci. Eng.* **2014**, *16*, 62−74.

DOI: 10.1021/acs.jpca.9b00816
J. Phys. Chem. A 2019, 123, 2843−2852